FULL PAPER

Seeing Hydrogen in Colors: Low-Cost and Highly Sensitive Eye Readable Hydrogen Detectors

Peter Ngene, Tsveta Radeva, Martin Slaman, Ruud J. Westerwaal, Herman Schreuders, and Bernard Dam**

There is a great interest in the development of reliable and low-cost hydrogen sensors for applications in the hydrogen economy, industrial processes, space application, detection of environmental pollution, and biomedical applications. Here, a new type of optical detector that indicates the presence of hydrogen in concentration range 5 ppm to 0.1 vol% H_2 merely by a reversible and tunable color change is reported. The device takes advantage of the reversible change in optical properties of a Pd-capped Y thin film upon exposure to H_2, while the color is tuned using the interference of light reflected between the Y and Pd layers. In this way, an eye-readable optical sensor that circumvents the need for electronics and external digital readouts is created. Using surface modifications, the performance of the H_2 detector in humid and oxygen rich environment is greatly improved. Therefore, the device has the potential to be used for chemical and also biochemical/biomedical H_2 sensing applications such as breathe hydrogen tests.

1. Introduction

The use of hydrogen (H_2) is expected to grow dramatically in the coming years due to the crucial role it is anticipated to play as the backbone of future energy systems based on renewable and sustainable resources.[1,2] H_2 is highly explosive in the presence of oxygen, with a lower flammability limit of 4 vol% in air; therefore its timely detection is an important safety issue. Monitoring of hydrogen concentration is also essential to nuclear reactor safety, space applications, coal mine operations and many other industrial process.[3] Hydrogen sensing also plays important role in medical diagnostics such as in a breathe H_2 test for the detection of lactose and sucrose intolerance, and for the detection of environmental pollution.[4–10] Therefore the development of reliable, sensitive and inexpensive H_2 sensors that can be used for variety of applications is of a great importance.

Conventional H_2 sensors based on metal-oxide chemiresistors, thermal conductors, catalytic and electrochemical processes are often bulky, operate mostly at high temperatures (100–300 °C), are in general expensive and suffer from poor selectivity towards H_2.[3,11] State of the art H_2 sensors are based on reversible changes in the electrical, optical and structural properties of nanostructured and /or thin films of certain metals (especially Pd and Pd-alloys) upon exposure to H_2.[3,12–21] These sensors operate at room temperature, are less bulky and more sensitive to H_2. Among this variety of contemporary H_2 sensors, the optical monitoring of H_2 is considered very attractive due to its inherent safe nature when compared to other techniques that require electrical contacts. It offers the additional advantage of remote, distributed and multiple H_2 sensing via optic fibers. Several optic fiber H_2 sensors based on interferometric, micro mirrors, evanescent field interaction, fiber Bragg Gratings, long period gratings and surface Plasmon resonance have been reported.[11,16–18,22–33] These optical H_2 sensors generally exhibit a good sensitivity. However despite being based on optical changes, they still require a light source, an optical fiber and electronic devices to convert the optical change into a readable output. This contributes substantially to the cost of the sensor. In addition, they suffer from cross sensitivity and poor selectivity especially in an oxygen and moisture environments such as in biochemical and biomedical H_2 sensing applications where low concentrations of H_2 need to be detected in the presence of both O_2 and H_2O.

Hydrogen detection based on the gasochromic properties of nano-structured WO_3[34–37] and NiO films coated with Pd or Pt catalysts have been demonstrated.[34–37] However, to the best our knowledge, all these sensors require a light source and electronic readout devices (spectrometers). Moreover they have a comparatively slow recovery time at room temperatures and therefore operate at elevated temperatures (typically, 80–200 °C). Furthermore, unlike optical sensors based on H_2 interaction with metal thin films, the coloration process of gasochromic sensors does not only depend on the H_2 pressure (or concentration) and temperature, but also on the initial water content of the gasochromic metal oxides.[36,38] This hampers the reproducibility and accurate quantification of the hydrogen pressure.[34–38]

Dr. P. Ngene, Dr. T. Radeva, Dr. R. J. Westerwaal, H. Schreuders, Prof. B. Dam
Materials for Energy Conversion and Storage (MECS)
Department of Chemical Engineering
Delft University of Technology
Julianalaan 136, 2628, BL, Delft, The Netherlands
E-mail: p.ngene@tudelft.nl; B.Dam@tudelft.nl
M. Slaman
Department of Physics and Astronomy
Vrije Universiteit Amsterdam
De Boelelaan 1081, NL-1081, HV, Amsterdam, The Netherlands

DOI: 10.1002/adfm.201303065

Here, we report on the realization of a novel optical H_2 detector that indicates the presence of H_2 merely by a reversible change in color. We exploit the reversible change in the reflectance of Y thin films on hydrogenation to the YH_2 and YH_3 phase respectively[39,40] to create a H_2 indicator with reversible and tunable color changes at certain thermodynamically determined pressure thresholds. The eye-readable change in color is the result of an interference effect and circumvents the need for an optic fiber and transducer or electrical readout. Using surface modifications, the selectivity is greatly enhanced such that, unlike many other H_2 sensors, it can detect very low H_2 concentrations (0.1% H_2/Ar) even in the presence of moisture, or/and oxygen. Therefore the device is very interesting for various applications such as H_2 leak detection, environmental pollution monitoring and biochemical/biomedical H_2 sensing purposes. The ability to fabricate the detector on cheap substrates such as plastics and paper makes it also appealing for disposable applications.

2. Results and Discussion

2.1. Configuration and Sensing Mechanism

The configuration and operation mechanism of our proposed H_2 detector is shown in **Figure 1**. The sensing layer is a thin film of Y sputtered on a 1 cm × 1 cm quartz substrate. On top of the Y is a 50 nm Pd thin film which serves as a (de) hydrogenation catalyst. The Pd layer also prevents oxidation of the Y[41] and enhances the observable colors through interference effects as will be explained in detail later. The Pd layer is coated with a 30 nm sputtered PTFE (polytetrafluoroethylene) which protects it from deterioration.[42,43] In the as-prepared state, Y is highly reflective. Therefore, when looking through a transparent substrate, nearly all the light falling on the Y is reflected as shown in Figure 1A. On exposure to H_2, Y turns into a semitransparent YH_2 phase at about 10^{-31} mbar. The semiconducting transparent YH_3 state is obtained at 0.1 mbar.[44,45] Pd is very reflective and therefore in the YH_x states, the reflection has a component from the substrate/YH_x and the YH_x/Pd interface as shown in Figure 1B (for a very smooth interfaces). The degree of constructive or destructive interference between the two light waves depends on the difference in their phase or optical path difference, which depends of course on the dielectric function of YH_x.

Stage 1 in Figure 1C shows the CCD camera image (without applying any image processing) of the as-prepared H_2 indicator layer geometry consisting of 60 nm Y, 50 nm Pd, and 30 nm PTFE (60Y/50Pd/30PTFE). On exposure 0.1 mbar H_2 partial pressure at room temperature, three different colors were observed. Upon dehydrogenation (by exposure to air or 20% O_2/Ar) the color changed from stage 4 directly to stage 2, thus skipping stage 3.

The observation of four different YH_x colors is surprising since from the presence of the three phases (Y, YH_2, and YH_3) we would expect three colors only. For more insight into the formation of the different colors, we followed the change in

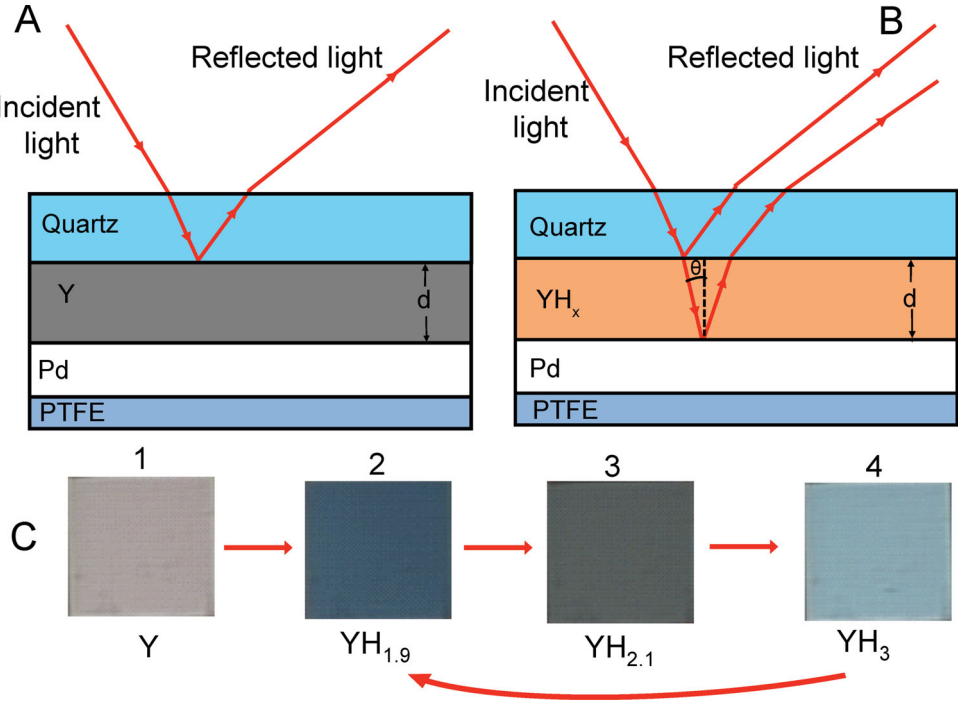

Figure 1. Configuration and operation mechanism of the H_2 detector: A) light reflection from Y layer in the as-prepared state, B) Interference effects due to optical changes when exposed to H_2. C) Change in color of the 60Y/50Pd/30PTFE H_2 indicator upon exposure to H_2 at room temperature, showing the four optical states Y → $YH_{1.9}$→ $YH_{2.1}$→ YH_3. Images were recorded with a CCD camera without involving image processing and therefore closely represent the visible impression.

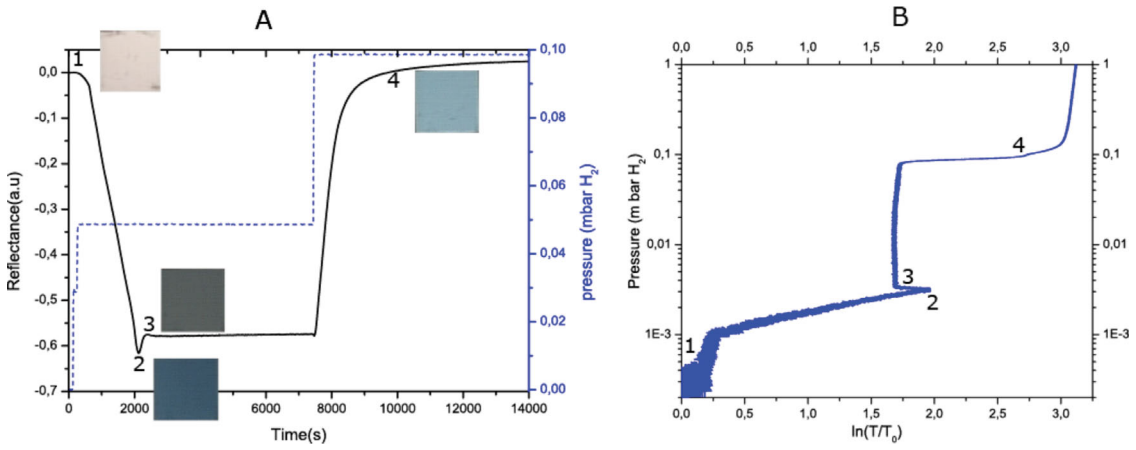

Figure 2. Change in optical properties of Y thin film at room temperature: A) change in reflectance of a 60 nm Y capped with a 50 nm Pd as a function of time and H_2 pressure. Inserted is the color associated with the different YH_x states when viewed through the substrate side. B) Pressure-transmission isotherm (PTI) of a 60 nm Y capped with 25 nm Pd. The plot shows the relationship between applied H_2 pressure and change in transmittance ($\ln(T/T_0)$) of the Y during H_2 absorption. T is the optical transmittance of the film during measurement while T_0 is the initial transmittance of the sample. The pressure was increased logarithmically from 0 to 1 mbar in 40 h. The four YH_x states are clearly seen in the two figures.

reflectance of the indicator as a function of time and pressure of H_2. **Figure 2**A shows that upon exposure to 0.05 mbar H_2, the reflectance of Y decreases quickly from its initial value (point 1) until it reaches a minimum at point 2, and increases slightly to point 3 where it stabilizes. Since the transition from Y to YH_2 is expected to occur far below 0.05 mbar,[44,45] we conclude that the two colors observed at point 2 and 3 are associated with the changes occurring within the YH_2 phase. It has been reported that the YH_2 phase allows for a hydrogen concentration range between $YH_{1.9}$ and $YH_{2.1}$. Within this fcc phase the optical properties are strongly dependent on the H_2 concentration.[40,45–47] $YH_{1.9}$ has a small transparency window at the red wavelengths [40,46,47] but on increasing the H_2 concentration from 1.9 to 2.1 the transmission decreases again.[46,47] While the dielectric function does not change much, the interference effect results in an improved optical contrast between the $YH_{1.9}$ and $YH_{2.1}$ states. When the pressure is increased to 0.1 mbar (which is the room temperature equilibrium pressure for the transition $YH_{2.1} \rightarrow YH_{2.7}$[44,45], the reflectance increases rapidly to point "4" which is almost equal to the reflectance of the pure Y metal. The increase in reflectance at point 4 is not expected as the hcp YH_3 phase is a large bandgap semiconductor. However, due to the high transmittance of the YH_3 phase, most of the light is reflected back from the interface with the metallic Pd layer. The relationship between the transmittance of Y and the H_2 concentration is shown in the pressure-transmission isotherm (PTI) in Figure 2B. A sloping plateau pressure corresponding to $Y \rightarrow YH_{1.9}$ is seen around 2×10^{-3} mbar. Since the equilibrium pressure for the transition of Y to $YH_{1.9}$ is at about 10^{-27} mbar, the fact that we observe this transition around 2×10^{-3} mbar is most likely due to the slow kinetics of the hydrogenation process. At the end of the plateau we observe a decrease in transmission (from "2" to "3") due to the formation of $YH_{2.1}$. From this point the transmission remains constant until the H_2 pressure reaches 0.1 mbar, at which the transmittance increases significantly due to the formation of the very transparent YH_3. In this case, the flat nature of the plateau indicates that this transition reflects the two-phase thermodynamic equilibrium between the dihydride and the trihydride phase. Note that for the transmission measurements, the thickness of the Pd was reduced to 25 nm to enhance transmission of light through the film.

The direct transition of YH_3 to $YH_{1.9}$ on dehydrogenation as seen in Figure 1C is in accordance with literature, which relates this hysteretic effect to the tensile strain developing in the Yttrium film on desorption.[48] Due to the low equilibrium pressure, a full desorption to the Y phase is possible only around 750 °C.[49] Thus, the subsequent hydrogenation of the detector is only possible from $YH_{1.9} \rightarrow YH_{2.1} \rightarrow YH_3$ and back. As shown in **Figure 3**A and 3B, the transition is highly reversible and can be repeated severally. Thus after the first hydrogenation cycle, we realized a three state H_2 detector that indicates the presence of H_2 by changing from deep blue ($YH_{1.9}$) to gray ($YH_{2.1}$) at concentrations below 0.1 mbar H_2 and to light blue (YH_3) at ≥0.1 mbar H_2. In practice the first color change ($YH_{1.9} \rightarrow YH_{2.1}$) is observed at hydrogen concentrations as low as 5 ppm (Figure S4 in Supporting Information).

2.2. Kinetics and Selectivity

The response time and selectivity are very important properties of H_2 sensors. **Figure 4** summarizes the response time (kinetics) and selectivity of the H_2 indicator in the presence of O_2 and H_2O, which are two major contaminant gases to be encountered in the various H_2 sensing applications. It is found that the time it takes our H_2 detector to change from one color to another generally depends on the H_2 concentration and the environmental conditions. Figure 4A shows that in H_2O and O_2 free environment, the transition $YH_{1.9}$ (peak) → $YH_{2.1}$(valley) → YH_3 (plateau) takes place in about 10 s for a 3% H_2/Ar gas mixture, and increases to 25 and 100 s for 1% and 0.12% H_2/Ar

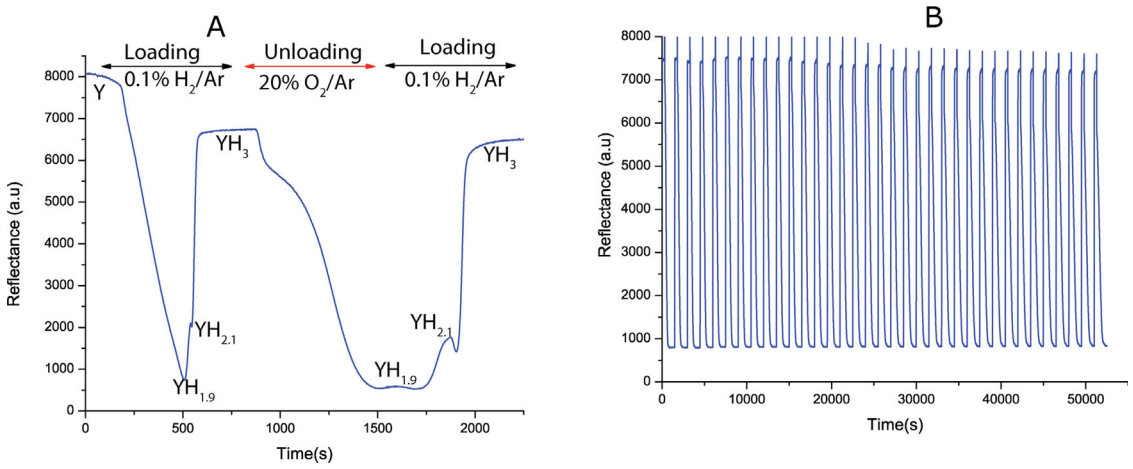

Figure 3. Performance of the H_2 detector in a flow of 150 mL min^{-1} H_2/gas mixtures. A) First and second hydrogenation/dehydrogenation cycles in 0.1% H_2/Ar for loading and 20% O_2/Ar for unloading. B) 40 cycles in 1% H_2/Ar, showing that the sensor is stable upon cycling.

respectively. Below 0.05% H_2, only one color change is observed ($YH_{1.9} \rightarrow YH_{2.1}$) and this color change is observed at a minimum pressure of 5 ppm H_2 with a long response time (≈30 min) as shown in Figure S4 (Supporting Information). However, it is important to note that the response time is the time taken to complete the color changing process associated with going from one YH*x* state to another, that is, the phase transition. A gradual change in color can already be visualized within 15 s as soon as hydrogen is introduced to the sample. Moreover, the time taken to complete the coloration decreases significantly as the concentration of hydrogen increases, as shown in Figure 4A. Thus the response time for the detector under O_2 and moisture free environments is adequate for many applications and comparable to state of the art H_2 sensors.[3,12–21] A fiber-optic hydrogen sensor based on the Mach–Zehnder interferometer had been realized with sensitivity of 2ppb H_2 in Ar, and a response time of 30 s.[22] However, the degree of complexity of the device made it relatively unattractive for practical hydrogen sensing applications.[31]

For the H_2 detector to be used for biochemical and biomedical applications, it should be able to detect down to 0.1–0.3% H_2 in the presence of O_2 and/or H_2O.[50] To this end we investigated the effect of O_2 and/or H_2O on the performance of the detector. Figure 4B indicates that in an environment that is almost saturated with water (97% relative humidity) the device can detect down to 2% H_2/Ar. However the kinetics is significantly reduced, for example the time to detect 4% H_2/Ar increases from about 10 s in moisture free environment to 1200 s in the presence of water. Similarly the presence of just 5% O_2 in the gas mixture adversely affects the performance of the indicator (Figure 4C) and is worse when both O_2 and H_2O are present, as seen for the 1% H_2+5% O_2 mixture at 97% relative humidity.

Dehydrogenation or unloading of the indicator ($YH_3 \rightarrow YH_{1.9}$) takes about 250 s in dry air or 20% O_2/Ar but the dehydrogenation time decreases in humid environments. This can be seen as an advantage in biochemical and biomedical applications. Hydrogen sensors/detectors based on H_2 sorption in metals generally suffer from a low sensitivity in the presence of O_2 and/or moisture especially at very low H_2 concentrations. This is due to competing reactions between adsorbed O_2 or hydroxyl groups (OH^-) and H_2 on the surface of the catalyst to form H_2O

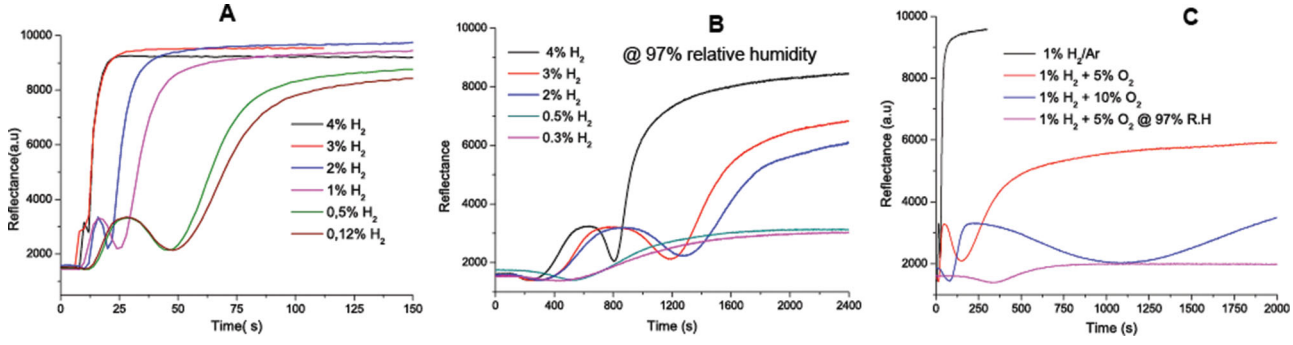

Figure 4. Kinetics and selectivity experiments showing the effects of O_2 and/or H_2O on the performance of the H_2 detector at room temperature and 150 mL min^{-1} total gas flow. A) Response to 4 – 0.12% H_2/Ar in O_2 and H_2O free environment. B) Response to 4 – 0.3% H_2/Ar bubbled through a moisturizer (95–97% Relative humidity, R.H). C) Addition of 5 and 10% O_2 to 1%H_2/Ar mixture significantly reduced sensor's response kinetics, and in the presence of both 5% O_2 and moisture (97% R.H) the sensor does not respond. Note that as $Y \rightarrow YH_{1.9}$ is not reversible, hence only the optical change on going from $YH_{1.9} \rightarrow YH_{2.1} \rightarrow YH_3$ is shown here.

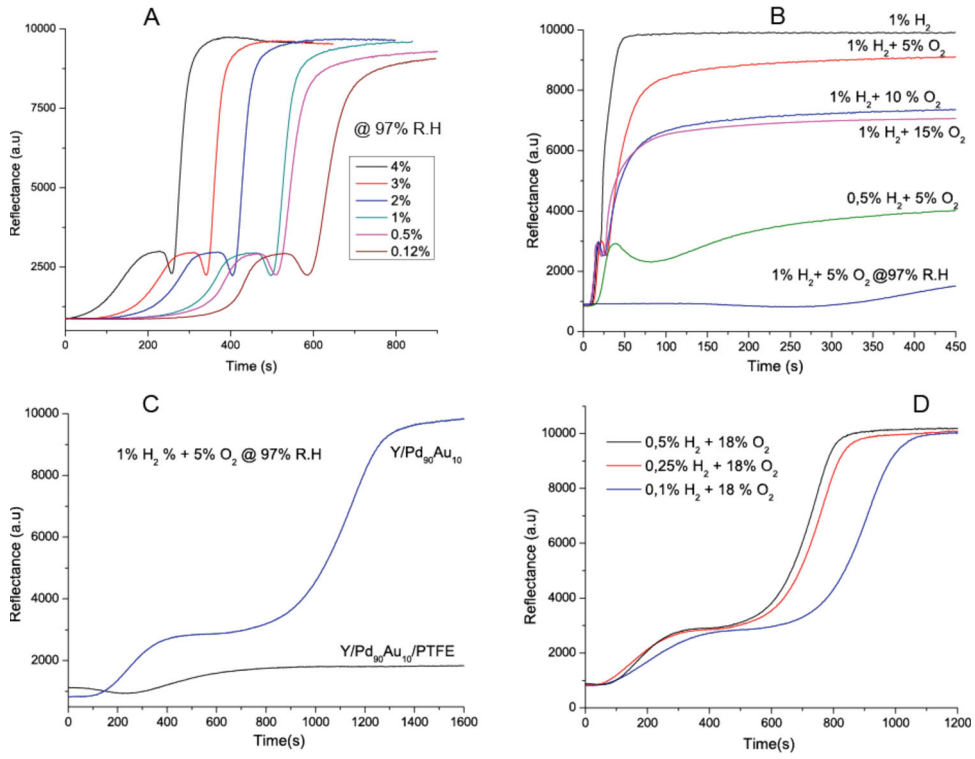

Figure 5. Effect of Au and PTFE on the kinetics and selectivity of the detector in presence of O_2 and H_2O. A) Response of a detector consisting of $Y/Pd_{90}/Au_{10}$/PTFE to a 150 mL min^{-1} flow of 4 – 0.12% H_2/Ar bubbled through a moisturizer (95–97% Relative humidity). B) The sample $Y/Pd_{90}/Au_{10}$/PTFE is able to detect 1% H_2 in the presence of up to 15% O_2 however in the presence of both O_2 and H_2O (97%RH) the response is highly retarded. C) Effect of PTFE on selectivity: unlike the PTFE containing samples, a detector without PTFE layer ($Y/Pd_{90}/Au_{10}$) is able to detect 1% H_2 in the presence of 5% O_2 and 97% RH. D) In the absence of H_2O, the detector without PTFE ($Y/Pd_{90}/Au_{10}$) is able to detect down to 0.1% H_2 in the presence of 18% O_2. Note, that only the optical changes on going from $YH_{1.9} \rightarrow YH_{2.1} \rightarrow YH_3$ can be detected reversibly.

instead of hydrogenating the sensing layer.[42,51] This is more severe in a humid environment because the presence of water increases the formation of hydroxyl groups (OH^-) which easily combine with a hydrogen atom to form water. In the next section we show how to modify this effect.

2.2.1. Enhancing Kinetics and Selectivity by Surface Modification

Our approach to enhance selectivity is to modify the surface chemistry by alloying the Pd catalyst with gold which has less affinity to adsorb O_2.[42,52] **Figure 5**A shows the response of a sample in which the Pd has been alloyed with 10% Au via co-sputtering of Pd and Au. Comparing Figure 4B and Figure 5A shows that the presence of Au significantly enhances the loading kinetics in a humid environment. Thus a 0.12% H_2/Ar mixture can be detected in an environment with 97% relative humidity. The sensor remains stable after 40 loading and unloading cycles under such conditions (Figures S5,S6 in the Supporting Information).

Figure 5A indicates that moisture has an effect only on the formation of the dihydride ($YH_{2.1}$) phase. The lower the H_2 concentration, the longer it takes for this onset of the hydrogenation to occur. However once the initial hydrogenation has occurred, the formation of YH_3 proceeds much faster, and hardly depends on the H_2 concentration in the range measured. As shown in Figure 5B, the addition of Au also improves the kinetics and selectivity of the detector towards H_2 in the presence of O_2. Unfortunately alloying with Au did not show any positive effects in the presence of both O_2 and H_2O as can be seen for the 1% H_2+ 5% O_2 @ 97% RH (Figure 5B). Surprisingly, omitting the PTFE layer of Au containing samples enhances the performance of the detector remarkably in the presence of both O_2 and H_2O (Figure 5C). Impressively, a detector with the configuration $Y/Pd_{90}Au_{10}$ (thus without a PTFE layer) detects 1% H_2 in the presence of 5% O_2 and 97% RH. Also very interesting is the fact that in the absence of moisture, this configuration detects down to 0.1% H_2 in the presence of 18% O_2 (atmospheric O_2 concentration) as shown in Figure 5D. This behaviour is maintained for environments containing up to 40% RH. Our results confirm the idea that alloying the Pd catalyst with Au significantly suppresses the adsorption of O_2 on the Pd–Au surface[52] thereby reducing the formation of H_2O. The decrease in hydrogenation or loading kinetics is expected since the presence of Au on the surface of the Pd will also result to fewer sites for the adsorption and dissociation of molecular H_2. The fact that the samples without a PTFE thin layer on the $Pd_{90}Au_{10}$ catalyst ($Y/Pd_{90}Au_{10}$) displayed better selectivity in presence of O_2 and/or H_2O than the ones containing PTFE ($Y/Pd_{90}Au_{10}$/PTFE), might imply that PTFE decreases the ability of Au to suppress the adsorption of O_2 on the Pd-Au surface. It has been reported that PTFE serves to protect the catalytic

layer of H_2 indicators from degradation.[42,43] However our results reveal that it also changes the surface chemistry especially at lower H_2 concentrations. Accordingly, we can tailor the performance of the H_2 indicator to different applications and environments by varying the concentration of Au in the catalytic layer and the type and thickness of the polymer protective coating (details to be published in a fourth coming article).

Although the response of the detector is slow in presence of both oxygen and water, to the best of our knowledge no hydrogen sensor has been shown to respond to such low concentration of hydrogen in the conditions shown above. The ability of the detector to detect H_2 in gas mixtures containing 0.1% H_2 and 18% O_2 makes it attractive as a simple and low-cost device for breathe analysis where the presence of up to 100 ppm H_2 in exhaled breathe is an indication of intestinal disorders such as malabsorption and intolerance to sucrose and lactose.[50] Similarly, the device is also suitable for use as a simple H_2 indicator in applications where the presence of hydrogen in ppm levels is an indication of environmental pollution, food decay and material deterioration.[3,8,53] Given that similar color change is observed when Y is deposited on cheap substrates such as papers, tapes and PET (Polyethylene terephthalate) foils (see Figure S1, Supporting Information), our H_2 detector can also be used as an inexpensive disposable device.

For application such as hydrogen breathe test for lactose intolerance, the exhaled breathe could be passed through an inexpensive device like silica gel that would reduce the moisture in the exhaled breathe prior to reaching the surface of the detector. The first color change would indicate the presence of H_2 in concentrations lower than 0.1% (not critical) while the second color change would indicate the presence of 0.1% H_2 and above (critical). Note that this is a threshold indicator, which might be used for a medical self-test. If the precise breathe H_2 concentration is required, a more elaborate electronic sensor will be needed. Note that CO_2 and volatile organic compounds (VOCs) such as, methane, acetone and toluene could be present at ppb or ppm levels in exhaled breathe, but Pd/Au has earlier been shown to be insensitive to CO_2, methane and ethane.[21] Since we use these layers as both catalyst and as protection layer for our Yttrium based device, we do not expect any cross-sensitivity due to these gasses. However CO and H_2S can cause a temporary poisoning of Pd based sensors and catalysts even at ppm levels. Therefore this could be an issue for application such as environmental H_2 monitoring (from food decay and material deterioration)

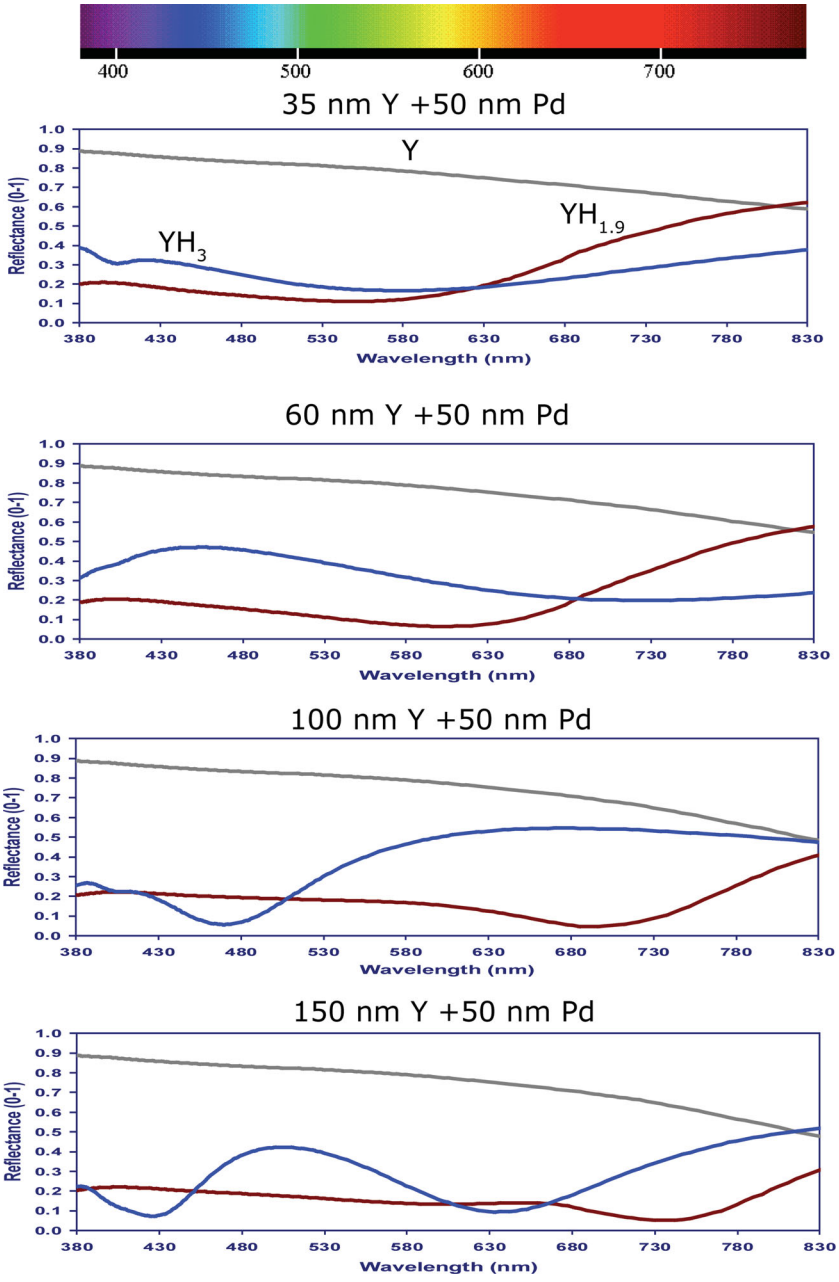

Figure 6. Optical simulation of the reflection at normal incidence of various Y films of different thickness deposited on a transparent substrate, and covered with a 50 nm Pd layer. Plotted is the "as deposited" reflection (top, gray), the loaded YH_3 phase (blue) and "unloaded" ($YH_{1.9}$) phase (red). The reflected color is the result of interference with the reflected light of the metallic Pd layer and can be selected by tuning the thickness of the Y layer.

2.3. Tuning the Colors of the Detector

To enhance the contrast of the detection colors, we investigated the effects of varying the Y thickness. An optical simulation of the detector's configuration with different Y thickness (**Figure 6**) shows that the reflectance of the different wavelengths of the white light is highly dependent on the Y thickness. While the reflection from the as-deposited Yttrium is hardly changed, the interference oscillations in the various phases are evident,

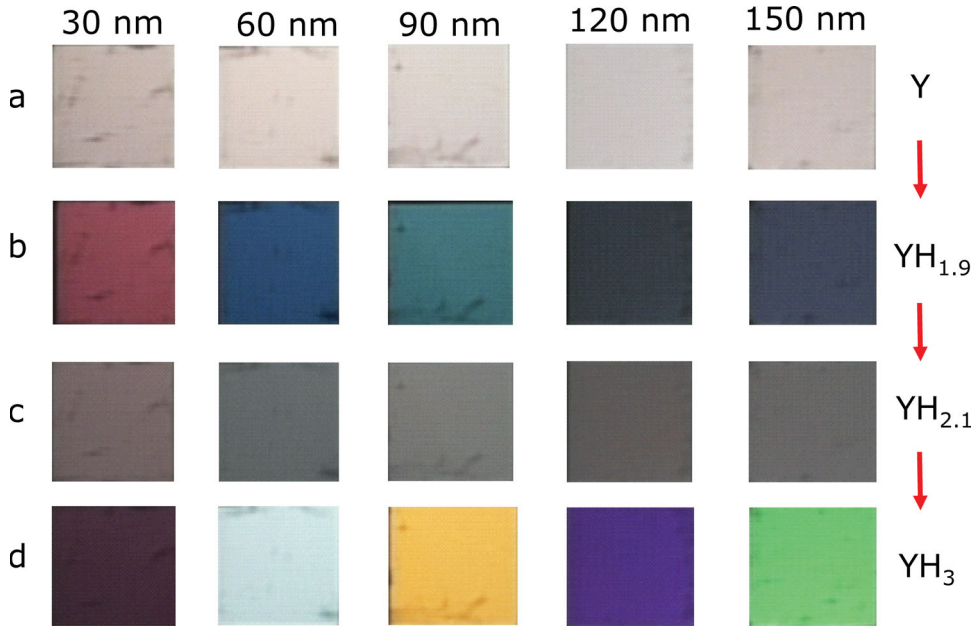

Figure 7. Apparent colors (recorded with a CCD camera) of the H_2 detector when viewed through the quartz substrate showing the effect of Y thickness on the observed color at the different hydrogenation states. a) As prepared, b) $YH_{1.9}$, c) $YH_{2.1}$, d) YH_3. All samples are capped by a 50 nm Pd thin film catalyst layer. Measurements were done at room temperature using 50 W halogen lamp light source and a Sony 3CCD Camera.

especially in the YH_3 phase. Due to a high absorption, the oscillations are less prominent in the $YH_{2.1}$ state.[46,47,54] **Figure 7** compares the colors of the H_2 detector with different Y thickness. Clearly, the as-deposited samples have a similar metallic appearance irrespective of the thickness of the Y film. Upon contact with H_2 we observe that the color of the indicator at each of the YH_x states depend strongly on the thickness of the Y film in line with the simulation results. The measured change in the reflectance of the samples as a function of the Y thickness is shown in Figure S2 (Supporting Information). A closer look at Figure 7C reveals that for $YH_{2.1}$, the indicators have similar color irrespective of the thickness. This can be understood on the basis of the metallic character of $YH_{2.1}$.[46,47,54] Clearly, the transparency of the $YH_{1.9}$ and YH_3 phases is on the other hand large enough to affect the mean free optical path of the light reflected at the YH_x/Pd interface. While in these experiments glass substrates were used, a similar optical behavior is observed when Y is deposited on plastics as shown in Figure S1 (Supporting Information). Even non-transparent substrates such as paper can be used for this purpose; however the layer geometry needs to be optimized in this case.

3. Conclusions

A novel and inexpensive hydrogen detector has been realized based on Y and Pd thin films deposited on transparent substrates. The change in the optical properties of Y thin films upon exposure to H_2 combined with interference effects between Y and Pd, allows us to create eye-visible effects. The detector is very simple to use as it indicates the presence of H_2 merely by a reversible and bright color change. Therefore it does not require an electronic readout device. Three different color states corresponding to three reversible hydrogenation states $YH_{1.9} \rightarrow YH_{2.1} \rightarrow YH_3$ are realized within the concentration range 5 ppm to 0.1% H_2. By changing the thickness of the Y thin film, the interference is influenced and thus the color of the detector can be tuned. The detector is very sensitive and can be used in a very simple way to warn people for the presence of H_2 in concentrations down to 5 ppm, which is far less than the lower explosion limit (4%) of H_2 in air.

While a PTFE protective coating increases the kinetics in the absence of O_2 and moisture, it decreases the selectivity of the detector in wet O_2, especially at low H_2 concentrations. Alloying 10% Au to the Pd (and without applying a PTFE coating) significantly improved the selectivity of the detector in the presence of O_2 and moisture. Thus the sample can detect 1% H_2 in the presence of 5% O_2 and saturated (97% relative humidity) environment. Furthermore, in moisture free environment (or less than 40% RH) the samples containing Au and without PTFE can detect down to 0.1% H_2 even in the presence of 18% O_2. This gives the H_2 indicator the potential to also be used in breathe H_2 analysis and other applications where low concentrations of H_2 need to be detected in the presence of O_2 and H_2O. This demonstrates that we have the opportunity to develop inexpensive, disposable eye-readable H_2 detectors/sensors for applications ranging from safety detection to biomedical applications.

4. Experimental Section

30–150 nm Y thin films were deposited at room temperature on 1 cm × 1 cm quartz substrates in an ultrahigh-vacuum (UHV) DC/

RF magnetron sputtering system with a base pressure 10^{-9} mbar, and deposition pressure of 0.003 mbar Ar. A 50 nm Pd or $Pd_{90}Au_{10}$ alloy thin film was deposited on top the Y film and a 30 nm polytetrafluorethylene (PTFE) was sputtered on top of the Pd (or Pd-Au) layer to minimize the effect of environmental contaminations on the surface. For deposition on non transparent substrate, the sputtering order is reversed so that the Y is deposited last. By exposure to air, about 3 nm native Y_2O_3 is formed which serves as a transparent medium for the light and also prevents further oxidation of the Y sensing layer. To measure the deposition rates, reference Y, Pd, and Au films were deposited independently by magnetron sputtering while monitoring the film growth over a well-defined time interval. By measuring the thickness of the reference films with a DekTak3 profilometer the deposition rate (nm s^{-1}) can be calculated. For co-sputtering of Pd and Au, the number of atoms of each element that arrive at the substrate per unit time and surface area, that is, the atomic ratio can be determined by using the atomic volumes of Pd (8.85 cm^3 mol^{-1}) and Au (10.2 cm^3 mol^{-1}) and their deposition rates. All targets used for this experiment have a purity of 99.9% (3N).

The surface morphology of the thin film at different stages was probed using atomic force microscope (AFM) in tapping (semi-contact) mode, while the microstructure characterized by X-ray diffraction (XRD) analysis using a Bruker D8 Advance XRD machine equipped with Co source (0.178897 nm). The optical response of the sensor during hydrogenation and dehydrogenation was monitored using Hydrogenography[55–57] both in reflection and transmission modes. In all measurements the samples are placed in a sample holder with the substrate side facing towards the CCD camera. The sample holder is then inserted into a closed cell with gas connections and the samples illuminated by a white light from halogen lamp. For reflection mode, the illumination is done on the substrate side while for transmission experiments it is done on the reverse (film) side. The reflected or transmitted signals, and the image of the sensor at a set time interval and pressure of hydrogen in the cell, were recorded with a CCD camera. The logarithm of the change in optical reflection $\ln(R/R_o)$ or transmittance $\ln(T/T_o)$, is related to the hydrogen concentration in the Y film. R and T are the reflection and transmittance respectively at any time while and R_o and T_o are the initial reflectance and transmittance of the sample.

A flow setup[21] is used for cycling measurements and to characterize the performance of the samples in the presence of both hydrogen and contaminants such as oxygen, moisture, N_2, CO_2 or any other gas of interest. A controlled gas flux of 150 mL min^{-1} containing H_2/Ar and any other gas of interest is mixed at certain ratios (using mass flow controllers) to achieve the desired concentrations. The gas mixture is passed through the sensor in a closed cell at room temperature. If desired, the gas stream is passed through a moisturizer (prior to entering the sample cell) equipped with a humidity probe so that the effect of moisture on sensor performance can also be evaluated. The outlet of the flow cell is connected to a gas-wash bottle filled with oil to prevent any backflow and thereby contamination of the sample. A tungsten halogen light source is guided towards the thin film using a multimode optical fiber. The reflected light from this layer is coupled to another fiber which is connected to an Ocean Optics USB4000 spectrometer. Light reflected by the hydrogen sensitive layer is measured by the spectrometer in the entire wavelength range from UV to near infrared. The flow set up data presented in this paper only show the reflectance at 635 nm wavelength for the 60 nm Y sample as it is a representative for the response of the 60 nm Y sample. The measurements are averaged over 5 data points to reduce the noise level.

Supporting Information

Supporting Information is available from the Wiley Online Library or from the author.

Acknowledgements

This work is financially supported by the Nederlandse Organisatie voor Wetenschappelijk Onderzoek (NWO) through the ACTS Sustainable Hydrogen program

Received: September 2, 2013
Revised: October 21, 2013
Published online: December 16, 2013

[1] A. Züttel, A. Borgschulte, L. Schlapbach, *Hydrogen as a future energy carrier*, Wiley-VCH, Weinheim, Germany **2008**.
[2] E. C. E. Rönnebro, E. H. Majzoub, *MRS Bull.* **2013**, *38*, 452.
[3] T. Hübert, L. Boon-Brett, G. Black, U. Banach, *Sens. Actuators, B* **2011**, *157*, 329.
[4] T. H. Risby, S. F. Solga, *Appl. Phys. B* **2006**, *85,* 421
[5] M. Nishibori, W. Shin, N. Izu, T. Itoh, I. Matsubara, *Sens. Actuators B* **2009**, *137*, 524.
[6] C. A. Grimes, K. G. Ong, O. K. Varghese, X. Yang, G. Mor, M. Paulose, E. C. Dickey, C. Ruan, M. V. Pishko, J. W. Kendig, A. J. Mason, *Sensors* **2003**, *3*, 69.
[7] S. Chong, A. Ramadan, E. Livesey, G. Wood, *Gastroenterology* **2002**, *122*, M1827.
[8] R. R. J. Maier, J. S. Barton, J. D. C. Jones, S. McCulloch, B. J. S. Jones, G. Burnell, *Meas. Sci. Technol.* **2006**, *17*, 1118.
[9] W. Shin, M. Nishibori, N. Izu, T. Itoh, I. Matsubara, K. Nose, A. Shimouchi, *Sens. Lett.* **2010**, *9*, 684.
[10] M. D. Levitt, *N. Engl. J. Med.* **1969**, *281*, 122.
[11] M. Ando, *Trends Anal. Chem.* **2006**, *25*, 937.
[12] X. Q. Zeng, Y. L. Wang, H. Deng, M. L. Latimer, Z. L. Xiao, J. Pearson, T. Xu, H. H. Wang, U. Welp, G. W. Crabtree, W. K. Kwok, *ACS Nano* **2011**, *5*, 7443.
[13] J. Lee, W. Shim, E. Lee, J. S. Noh, W. Lee, *Angew. Chem. Int. Ed.* **2011**, *50*, 5301.
[14] C. McDonagh, C. S. Burke, B. D. MacCraith, *Chem. Rev.* **2008**, *108*, 400.
[15] E. Lee, J. Lee, J. S. Noh, W. Kim, T. Lee, S. Maeng, W. Lee, *Int. J. Hydrogen Energy* **2012**, *37*, 14702.
[16] R. R. J. Maier, B. J. S. Jones, J. S. Barton, S. McCulloch, T. Allsop, J. D. C. Jones, I. Bennion, *J. Opt. A: Pure Appl. Opt.* **2007**, *9*, S45.
[17] C. Perrotton, N. Javahiraly, M. Slaman, B. Dam, P. Meyrueis, *Opt. Express* **2011**, *19*, A1175.
[18] C.-L. Tien, H.-W. Chen, W.-F. Liu, S.-S. Jyu, S.-W. Lin, Y.-S. Lin, *Thin Solid Films* **2008**, *516*, 5360.
[19] M. A. Butler, *Appl. Phys. Lett.* **1984**, *45*, 1007.
[20] F. A. Lewis, *Int. J. Hydrogen Energy* **1996**, *21*, 461.
[21] R. J. Westerwaal, J. S. A. Rooijmans, L. Leclercq, D. G. Gheorghe, T. Radeva, L. Mooij, T. Mak, L. Polak, M. Slaman, B. Dam, T. Rasing, *Int. J. Hydrogen Energy* **2013**, *38*, 4201.
[22] M. A. Butler, D. S. Ginley, *J. Appl. Phys.* **1988**, *64*, 7.
[23] X. Bévenot, A. Trouillet, C. Veillas, H. Gagnaire, M. Clément, *Meas. Sci. Technol.* **2002** *13*, 118.
[24] B. Chadwick, M. Gal, *Appl. Surf. Sci.* **1993**, *68*, 135.
[25] C. Perrotton, R. J. Westerwaal, N. Javahiraly, M. Slaman, H. Schreuders, B. Dam, P. Meyrueis, *Opt. Express* **2013**, *21*, 382.
[26] M. Tabib-Azar, B. Sutapun, R. Petrick, A. Kazemi, *Sens. Actuators B* **1999**, *56*, 158.
[27] A. Trouillet, E. Marin, C. Veillas, *Meas. Sci. Technol.* **2006**, *17*, 1124.
[28] J. Villatoro, D. Luna-Moreno, D. Monzón-Hernández, *Sens. Actuators B* **2005**, *110*, 23.
[29] J. Villatoro, D. Monzón-Hernández, *Opt. Express* **2005**, *13*, 5087.
[30] X. Wei, T. Wei, H. Xiao, Y. S. Lin, *Sens. Actuators B* **2008**, *134*, 687.

[31] S. F. Silva, L. Coelho, O. Frazao, J. L. Santos, F. X. Malcata, *IEEE Sens. J.* **2012**, *12*, 93.
[32] O. S. Wolfbels, *Anal. Chem.* **2008**, *80*, 4269.
[33] X. D. Wang, O. S. Wolfbeis, *Anal. Chem.* **2013**, *85*, 487.
[34] K. Ito, T. Ohgami, *Appl. Phys. Lett.* **1992**, *60*, 938.
[35] K. Takano, A. Inouye, S. Yamamoto, M. Sugimoto, M. Yoshikawa, S. Nagata, *Jpn. J. Appl. Phys., Part 1* **2007**, *46*, 6315.
[36] M. H. Yaacob, M. Breedon, K. Kalantar-zadeh, W. Wlodarski, *Sens. Actuators B* **2009**, *137*, 115.
[37] M. H. Yaacob, J. L. Campbell, A. Wisitsoraat, W. Wlodarski, *Sens. Lett.* **2011**, *9*, 898.
[38] A. Georg, W. Graf, R. Neumann, V. Wittwer, *Thin Solid Films* **2001**, *384*, 269.
[39] J. N. Huiberts, R. Griessen, J. H. Rector, R. J. Wijngaarden, J. P. Dekker, D. G. de Groot, N. J. Koeman, *Nature* **1996**, *380*, 231.
[40] F. J. A. den Broeder, S. J. van der Molen, M. Kremers, J. N. Huiberts, D. G. Nagengast, A. T. M. van Gogh, W. H. Huisman, N. J. Koeman, B. Dam, J. H. Rector, S. Plota, M. Haaksma, R. M. N. Hanzen, R. M. Jungblut, P. A. Duine, R. Griessen, *Nature* **1998**, *394*, 656.
[41] J. N. Huiberts, J. H. Rector, R. J. Wijngaarden, S. Jetten, D. De Groot, B. Dam, N. J. Koeman, R. Griessen, B. Hjarvarsson, S. Olafsson, Y. S. Cho, *J. Alloys Compd.* **1996**, *239*, 158.
[42] M. Slaman, B. Dam, H. Schreuders, R. Griessen, *Int. J. Hydrogen Energy* **2008**, *33*, 1084.
[43] M. Slaman, B. Dam, M. Pasturel, D. M. Borsa, H. Schreuders, J. H. Rector, R. Griessen, *Sens. Actuators B* **2007**, *123*, 538.
[44] R. Griessen, J. N. Huiberts, M. Kremers, A. T. M. Van Gogh, N. J. Koeman, J. P. Dekker, P. H. L. Notten, *J. Alloys Compd.* **1997**, *253–254*, 44.
[45] E. S. Kooij, A. T. M. van Gogh, R. Griessen, *J. Electrochem. Soc.* **1999**, *146*, 2990.
[46] J. H. Weaver, R. Rosei, D. T. Peterson, *Phys. Rev. B* **1979**, *19*, 4855.
[47] M. Kremers, N. J. Koeman, R. Griessen, P. H. L. Notten, R. Tolboom, P. J. Kelly, P. A. Duine, *Phys. Rev. B* **1998**, *57*, 4943.
[48] E. S. Kooij, A. T. M. Van Gogh, D. G. Nagengast, N. J. Koeman, R. Griessen, *Phys. Rev. B* **2000**, *62*, 10088.
[49] J. Hayoz, S. Sarbach, T. Pillo, E. Boschung, D. Naumovi, P. Aebi, L. Schlapbach, *Phys.Rev. B* **1998**, *58*, R4270.
[50] R. G. Barr, J. B. Watkins, J. A. Perman, *Pediatrics* **1981**, *68*, 526.
[51] L. G. Petersson, H. M. Dannetun, I. Lundström, *Surf. Sci.* **1985**, *161*, 77.
[52] A. Staykov, T. Kamachi, T. Ishihara, K. Yoshizawa, *J. Phys. Chem. C* **2008**, *112*, 19501.
[53] R. Nandi, S. Sengupta, *Crit. Rev. Microbiol.* **1998**, *24*, 61.
[54] A. T. M. van Gogh, D. G. Nagengast, E. S. Kooij, N. J. Koeman, J. H. Rector, R. Griessen, C. F. J. Flipse, R. Smeets, *Phys. Rev. B* **2001**, *63*.
[55] R. Gremaud, C. P. Broedersz, D. M. Borsa, A. Borgschulte, P. Mauron, H. Schreuders, J. H. Rector, B. Dam, R. Griessen, *Adv. Mater.* **2007**, *19*, 2813.
[56] R. Gremaud, M. Slaman, H. Schreuders, B. Dam, R. Griessen, *Appl. Phys. Lett.* **2007**, *91*.
[57] R. J. Westerwaal, C. Den Besten, M. Slaman, B. Dam, D. E. Nanu, A. J. Böttger, W. G. Haije, *Int. J. Hydrogen Energy* **2012**, *36*, 1074.